ACS OMEGA

Article

http://pubs.acs.org/journal/acsodf

New Mechanistic Insights: Why Do Plants Produce Isoprene?

Nassim Zeinali, Mohammednoor Altarawneh,* Dan Li, Jomana Al-Nu'airat, and Bogdan Z. Dlugogorski

School of Engineering and Information Technology, Murdoch University, 90 South Street, Murdoch, Western Australia 6150, Australia

Supporting Information

ABSTRACT: In this article, we argue that the primary role of isoprene is to remove the singlet delta oxygen (O_2 $^1\Delta_g$) that forms inside plants by ultraviolet excitation rather than to provide heat protection or scavenge ozone, OH, or other reactive oxygen species (ROS) in the gas phase. By deploying a quantum chemical framework, we address for the first time the exact mode of isoprene reactions with O_2 $^1\Delta_g$, the most prominent ROS that causes damage to leaves. Initial reactions of isoprene with O_2 $^1\Delta_g$ comprise its addition at the two terminal carbon atoms. The two primary open-shell adducts that appear in these reactions undergo 1,2-cycloaddition to generate methyl vinyl ketone and methacrolein, the sole products detected from in-house (i.e., inside of plants) oxidation of isoprene. Formation of other products, comprising the peroxy O−O bonds, is kinetically insignificant. Furthermore, these adducts are thermodynamically too unstable to diffuse outside of plants. Oxidation of isoprene with O_2 $^1\Delta_g$ does not produce new ROS (such as OH or HO_2), supporting the well-documented role of isoprene as an effective ROS scavenger. Deploying a solvation model reduces the energy requirements for the primary pathways in the range of 10−56 kJ/mol. The present results indicate that plants attach significant value to the in-home protection against O_2 $^1\Delta_g$ by investing carbon and energy into the formation of isoprene, in spite of the appearance of the cytotoxic methyl vinyl ketone as one of the reaction products. (The same chemical species also form in unrelated gas-phase reactions involving isoprene and other ROS.) This finding explains the primary reason for the appearance of the dynamic biosphere−atmosphere exchange of methyl vinyl ketone.

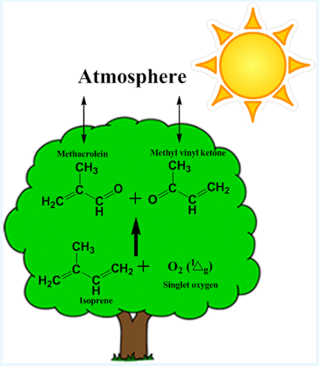

1. INTRODUCTION

Emission of isoprene (2-methyl-1,3-butadiene) from many terrestrial plants accounts for nearly one-third of the annual global budget of volatile organic compounds (VOCs) from all biogenic and anthropogenic sources combined.[1] Owing to its high chemical reactivity, once emitted to the atmosphere, isoprene plays a crucial role in many atmospheric phenomena.[2] This includes modifying the mechanisms of the atmospheric removal of other VOCs, influencing the formation of secondary organic aerosol and affecting the production of ozone. Although isoprene exerts no greenhouse gas (GHG) effect on its own right, its fast reaction with OH radicals can change the atmospheric oxidation capacity and the atmospheric lifetime of methane (the third most important GHG). But this is not the reason why plants invest their carbon and energy resources to synthesize isoprene.

A significant debate has been sweeping the field on reasons for plants to produce isoprene in an operation that is both biochemically expensive and energy dependent.[3] Mounting experimental evidence demonstrates that isoprene undergoes complex heat-tolerant mechanisms in plants. The direct production of isoprene from light-dependent photosynthesis indicates a plausible thermoslike protection of leaves from certain types of heat shocks.[4] However, the most discussed role of isoprene is the mitigation of the effect of reactive oxygen species (ROS) in plants.[5] By acting as an ROS scavenger, isoprene can prevent visible damage caused by exposure of leaves to ozone or OH radicals and reduce the loss in their photosynthetic capacity. Nonetheless, isoprene−ROS reactions remain to be elucidated, especially those occurring inside plants.

The lowest excited state of singlet delta oxygen (O_2 $^1\Delta_g$) constitutes the most prominent ROS causing damage to leaves[6] in such a way that this exotic species accounts for over 80% of lipid oxidation within leaf tissues.[7] Photo-induced activation produces O_2 $^1\Delta_g$ in plants, mainly mediated by the excited state of the triplet chlorophyll (^{3}Chl*).[8] The literature has documented well the O_2 $^1\Delta_g$ scavenging properties of isoprene.[9] Isoprene acts as an effective quenching agent for many ROS, including the O_2 $^1\Delta_g$.[3b] Through the use of rose bengal as a photo-sensitizer, experiments[9a,b] have demonstrated that isoprene protects plants against the damaging effect of O_2 $^1\Delta_g$. In fact, ultraviolet (UV) excitation of an isoprene/ground state oxygen mixture results in the formation of O_2 $^1\Delta_g$.[10] Because the biochemical synthesis of isoprene displays light-dependency, the resistance to O_2 $^1\Delta_g$ correlates positively with the light intensity.[3a] However, the exact mode of isoprene attacks on O_2 $^1\Delta_g$ remains largely unclear. Jardine et al.[11] have experimentally simulated a "within-plant" oxidation process of isoprene to report methyl vinyl ketone and methacrolein as the sole oxidation products. The authors linked the formation of

Received: April 24, 2016
Accepted: August 4, 2016
Published: August 18, 2016

DOI: 10.1021/acsomega.6b00025
ACS Omega 2016, 1, 220−225

these two compounds with the functionality of isoprene as an ROS scavenger but without pointing to $O_2\ ^1\Delta_g$, in particular.

Here, we suggest that the main role of isoprene is to remove $O_2\ ^1\Delta_g$ that forms inside of plants by the photo-induced activation process. From this perspective, by deploying quantum chemical calculations, this article provides a detailed mechanistic account of the reactions of $O_2\ ^1\Delta_g$ with isoprene. Because of the highly transient nature of $O_2\ ^1\Delta_g$ (lifetime of a few microseconds),[12] the reaction chemistry of $O_2\ ^1\Delta_g$ constitutes an excellent candidate for a purely theoretical scrutiny. The reaction mechanism and the kinetic parameters developed herein will assist in formulating an atomic-scale understanding of the protective functions of isoprene in plants against ROS, particularly $O_2\ ^1\Delta_g$.

2. METHODOLOGY

Normally, treatment of the biradical character exhibited by the adduct of isoprene and $O_2\ ^1\Delta_g$ would require the application of multireference wave function methods such as CASSAF and CASSTP2.[13] The pioneering work by the Yamaguchi[14] group has demonstrated that the energies of the biradical systems computed by any single-determinant method can be significantly improved by the application of a simple approximate spin-projection (AP) scheme. In this scheme, an approximate spin-projected energy (E^{AP}) can be derived from the energies of the broken-symmetry (E^{BS}) and pure high-spin (E^{HS}) states

$$E^{AP} = f^{AP}E^{BS} - (f-1)E^{HS}$$

where f^{AP} denotes the spin-projection factor,

$$f^{AP} = \frac{\langle S^2\rangle^{HS} - s(s+1)}{\langle S^2\rangle^{HS} - \langle S^2\rangle^{BS}}$$

and $\langle S^2\rangle^{HS}$ and $\langle S^2\rangle^{BS}$ signify the expectation values of spin contamination pertinent to the pure high-spin and broken-symmetry states, respectively. Application of the AP methodology to various biradical systems yields B3LYP-derived energies to within 4.2−12.6 kJ/mol of the corresponding values obtained with more expensive multireference methods.[15] In a series of contributions,[16] Cremer and co-workers showed that unrestricted density functional theory (UDFT) methods perform surprisingly well in deriving energies and geometries of singlet biradicals.

Accordingly, we deploy the density functional theory (DFT) functional of B3LYP with the extended 6-311+G(d,p)[17] basis set to investigate the biradical system of isoprene and $O_2\ ^1\Delta_g$. Final energies are corrected using the AP approach as described above, whenever the reacting species (including reactants, products, and transition states) attain a biradical character. As an initial accuracy benchmark, we calculate the triplet−singlet delta enthalpic gap of the oxygen molecule to be 85.4 kJ/mol, in a relatively good agreement with the corresponding experimental value at 94.1 kJ/mol.[12] Standard UB3LYP calculations result in a significantly larger enthalpy gap of 161.5 kJ/mol, demonstrating the necessity of applying the AP approach. Table S1 enlists the calculated thermal enthalpies and the expected spin contamination values, that is, values required in calculations based on the AP methodology. We carry out all structural optimizations and energy calculations using the Gaussian 09 suite of programs.[18] We have carefully confirmed the identity of each transition structure by performing intrinsic reaction coordinate (IRC) calculations.

The ChemRate code facilitates the calculation of the reaction rate constants, in the temperature range of 300−600 K.[19] We obtain the Fukui[20] indices for electrophilic attack (f^1) and the electronic Hirshfeld[21] charges with the aid of DMol^3 code.[22] The Fukui f^{-1} indices serve as a molecular descriptor, reflecting the tendency of a certain site in a chemical species to undergo an electrophilic addition.

3. RESULTS AND DISCUSSION

The structure of isoprene features a conjugated π system, where the digits 1 and 2 denote two sites for the addition of $O_2\ ^1\Delta_g$

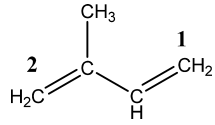

Figure 1. Isoprene chemical structure.

(Figure 1). Figure 2 depicts the mechanism of the reactions of isoprene with $O_2\ ^1\Delta_g$, with the geometries of intermediates and transition structures portrayed separately in Figures S1 and S2. The electrophilic properties of $O_2\ ^1\Delta_g$ enable the introduction of oxygen atoms into olefins, dienes, and aromatic structures through three main categories of reactions: 1,2-cycloaddition to double bonds, 1,4-cycloaddition to aromatic rings, and the so-called concerted ene reaction. Generally,[23] the nonconcerted mechanism underlying the reactions of typical dienes with the $O_2\ ^1\Delta_g$ passes through diradical intermediates. For instance, the diradical peroxy adduct has been previously observed in the case of *cis*-1,3-butadiene.[13b] Similarly, in this study, the simulations led to two diradical intermediates (M_1 and M_{14}).

All attempts to locate the transition structures preceding 1,2-/1,4-cyloadditions or a direct abstraction of a methyl hydrogen atom (i.e., an ene reaction) converge to the peroxy adducts M_1 and M_{14}, in which the oxygen molecule binds to the terminal carbon atoms at sites 1 and 14, respectively. If it operates in our system, ene reaction should result in the formation of an allylic hydroperoxide upon a shift in the position of the most electron-rich double bond (i.e., species M_3 in Figure 2). If the occurrence of an ene is a feasible opening channel, this would violate the role of isoprene as an ROS scavenger because it results in the generation of another potent ROS species, namely the OH radical, through dissociation of the weak O−OH bond.

Although peroxirane and zwitterionic intermediates were detected on the potential energy surface in the reaction between butadiene and $O_2\ ^1\Delta_g$,[24] despite our best efforts, we were unable to locate these intermediates. Nonetheless, conversion of the initially formed diradical peroxy-type adduct into peroxirane was shown to be a highly endothermic process by about 100 kJ/mol. Analogously, a related study[25] predicted that a zwitterionic adduct resides nearly 40 kJ/mol above the initially formed diradical intermediates.

Rotation of the peroxy O−O bond in M_1 and M_{14} adducts could potentially generate *syn* and *anti* conformers. However, performing a partial optimization along the corresponding dihedral angles leads to structures in which the outer oxygen atom either abstracts a hydrogen atom or adds to the carbon skeleton (one of the products in Figure 2); viz., stable *syn* and *anti* conformers do not arise in M_1 and M_{14}.

The M_1 and M_{14} moieties, in addition to their transition structures TS_1 and TS_{12}, possess an open-shell character. On

DOI: 10.1021/acsomega.6b00025
ACS Omega 2016, 1, 220−225

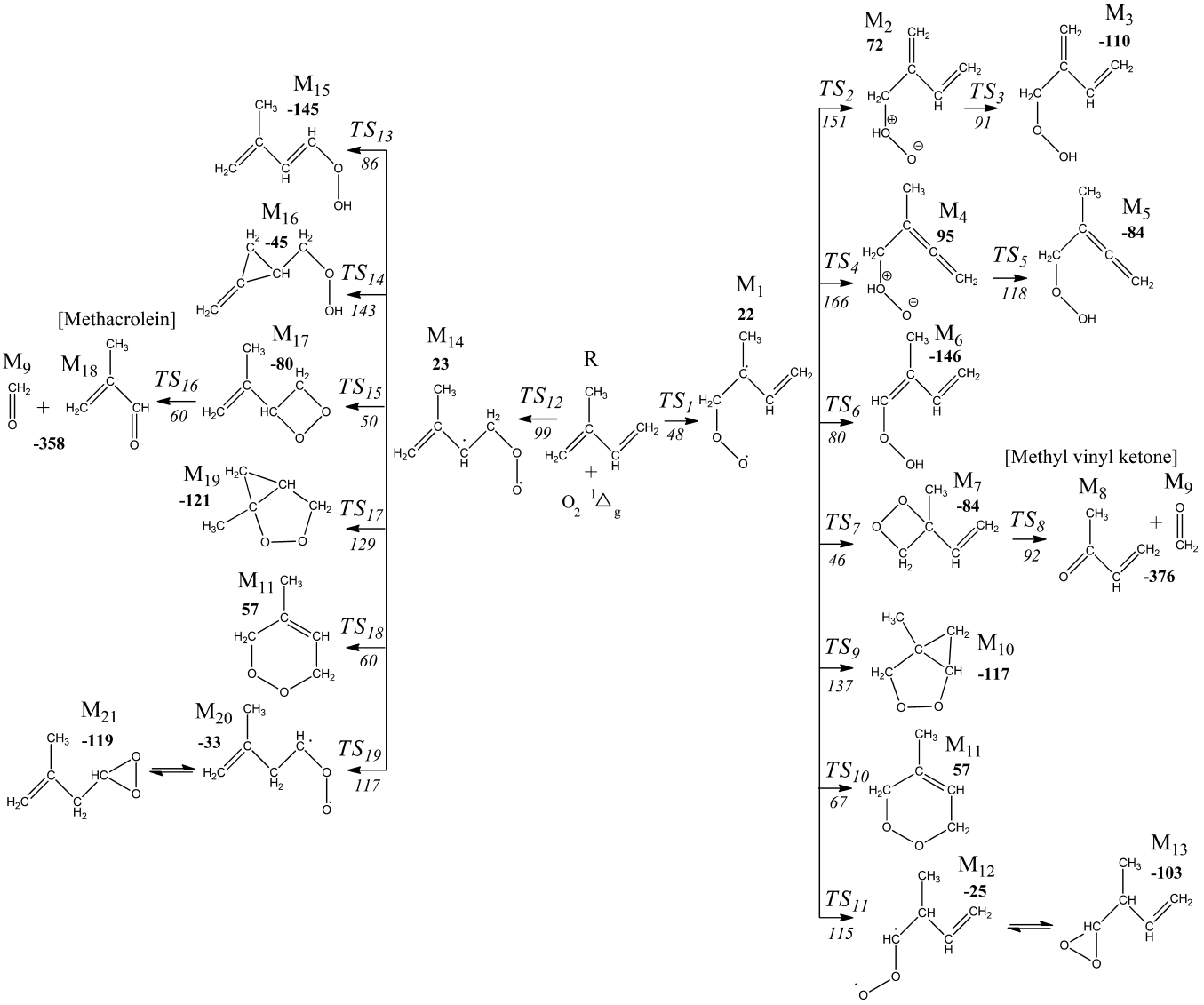

Figure 2. Reaction routes in the isoprene + O_2 $^1\Delta_g$ system obtained by the calculation level of B3LYP/6-311+G(d,p). The values in bold and italics signify reaction and activation enthalpies computed at 298.15 K, respectively (in kJ/mol).

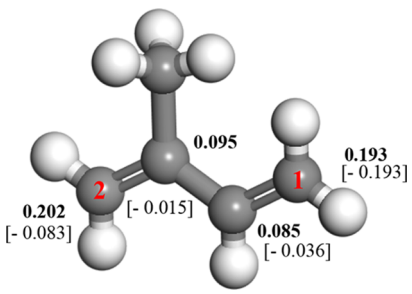

Figure 3. Fukui f^{-1} indices (in bold) and Hirshfeld charges (in brackets).

the basis of AP-corrected enthalpies (298.15 K), the reaction barrier of TS_{12} (99 kJ/mol) overshoots that of TS_1 by 51 kJ/mol. To elucidate the different reactivities for the addition of O_2 $^1\Delta_g$ at sites 1 and 2, Figure 3 displays the calculated Fukui indices and electronic charges on isoprene. The higher electron densities and f^{-1} values at site 2 in comparison with the analogous estimates at site 1 concur with the lower activation barrier of TS_1 with reference to TS_{12}.

The two initial adducts, M_1 and M_{14}, reside at a similar level above the entrance channel. As Figure 2 depicts, the initial adduct M_1 branches into seven exit routes, whereas M_{14} launches six channels. In the main channel, a 1,2-cycloaddition occurs via TS_7 overcoming a modest enthalpic barrier of 46 kJ/mol and forms the M_7 adduct. A very exothermic C−C bond fission (−376 kJ/mol) in M_7 provides the experimental product for in-house oxidation of isoprene, the methyl vinyl ketone molecule. This process takes place through a barrier of 92 kJ/mol embedded in TS_8.

The transition states TS_2, TS_4, and TS_6 from the main channel, along with TS_{13} and TS_{14} signify H-migration reactions, in which the outer oxygen atom abstracts a hydrogen atom from the neighboring carbon atoms through sizable reaction barriers amounting to 151, 166, 80, 86, and 143 kJ/mol, respectively. Fission of the relatively weak O−OH bond in the structure of hydroperoxide intermediates (such as M_5 and M_{16}) requires modest bond dissociation enthalpies in the range of 141−147 kJ/mol. Nonetheless, significantly higher barriers for the formation of allylic hydroperoxide (80−166 kJ/mol) with reference to the barrier of the main route (46 kJ/mol)

DOI: 10.1021/acsomega.6b00025
ACS Omega 2016, 1, 220−225

Table 1. Arrhenius Parameters for Reactions Encountered during Oxidation by O_2 $^1\Delta_g$

reaction	A (s^{-1} or cm^3 $molecule^{-1}$ s^{-1})	E_a (kJ/mol)
isoprene + O_2 $^1\Delta_g$ → M_1	2.60×10^{-12}	55
M_1 → M_2	2.36×10^{12}	132
M_2 → M_3	4.55×10^{13}	22
M_1 → M_4	1.22×10^{13}	147
M_4 → M_5	1.80×10^{13}	26
M_1 → M_6	1.17×10^{13}	61
M_1 → M_7	2.58×10^{12}	27
M_7 → M_8 + M_9	3.51×10^{13}	180
M_1 → M_{10}	1.24×10^{12}	118
M_1 → M_{11}	8.17×10^{11}	48
M_1 → M_{12}	1.37×10^{13}	96
isoprene + O_2 $^1\Delta_g$ → M_{14}	1.16×10^{-12}	105
M_{14} → M_{15}	1.39×10^{13}	66
M_{14} → M_{16}	1.69×10^{12}	122
M_{14} → M_{17}	4.88×10^{12}	29
M_{17} → M_{18} + M_9	2.55×10^{13}	143
M_{14} → M_{19}	1.31×10^{12}	108
M_{14} → M_{20}	2.47×10^{12}	39
M_{14} → M_{21}	1.88×10^{13}	97

indicate that the formation of the propagating OH radical from the unimolecular rearrangement of M_1 is highly unlikely. All our attempts to find transition states connecting M_1 directly with M_3 and M_5 have led to TS_2 and TS_4, respectively. This interpretation has been guided by detailed IRC calculations and vibration analysis. The formation of hydroperoxide M_6 from M_1, as well as M_{15} from M_{14}, occurs via H abstraction from the CH_2 site by the terminal oxygen atom of the peroxy group, with modest reaction barriers of 80 kJ/mol (TS_7) and 86 kJ/mol (TS_{14}), respectively.

Transition structures TS_9 (137 kJ/mol) and TS_{10} (67 kJ/mol) engender 1,3- and 1,4-cycloadditions commencing from M_1. Formation of the six-membered ring, M_{11} structure, from M_1 and M_{14} proceeds via similar reaction barriers through TS_{10} and TS_{18}. The peroxy O−O bonds in the molecules are typically very weak, that is, 150 kJ/mol.[26] This explains the absence of M_{10}, M_{11}, and M_{19} from the products of isoprene oxidations initiated by O_2 $^1\Delta_g$.

Both M_1 and M_{14} are capable of forming short-lived dioxirane species M_{13} and M_{21} via a two-step pathway, initiated by 1,2-hydrogen transfer characterized by the TS_{11} (115 kJ/mol) and TS_{19} (117 kJ/mol) transition states. The corresponding biradical intermediates of M_{12} and M_{20} then pass through a barrierless unimolecular cyclization to form the highly stable heterocyclic peroxides M_{13} and M_{21}. Because the reaction barriers associated with TS_{11} and TS_{19} significantly overshoot the barriers of the primary channels (TS_7 and TS_{15}), synthesis of dioxiranes from the reaction of isoprene with O_2 $^1\Delta_g$ is largely negligible.

On the basis of the reaction and activation barriers displayed in Figure 2, the channel associated with the attack of O_2 $^1\Delta_g$ molecule on the double bond at site 2 produces methyl vinyl ketone predominantly. Likewise, addition of oxygen at site 1 preferentially forms the second experimentally detected product of methacrolein. The kinetic parameters listed in Table 1 reveal that the overall isoprene + O_2 $^1\Delta_g$ reaction proceeds mainly by the addition of O_2 $^1\Delta_g$ at site 2 (M_1) and forms methyl vinyl ketone molecule in a three-step mechanism

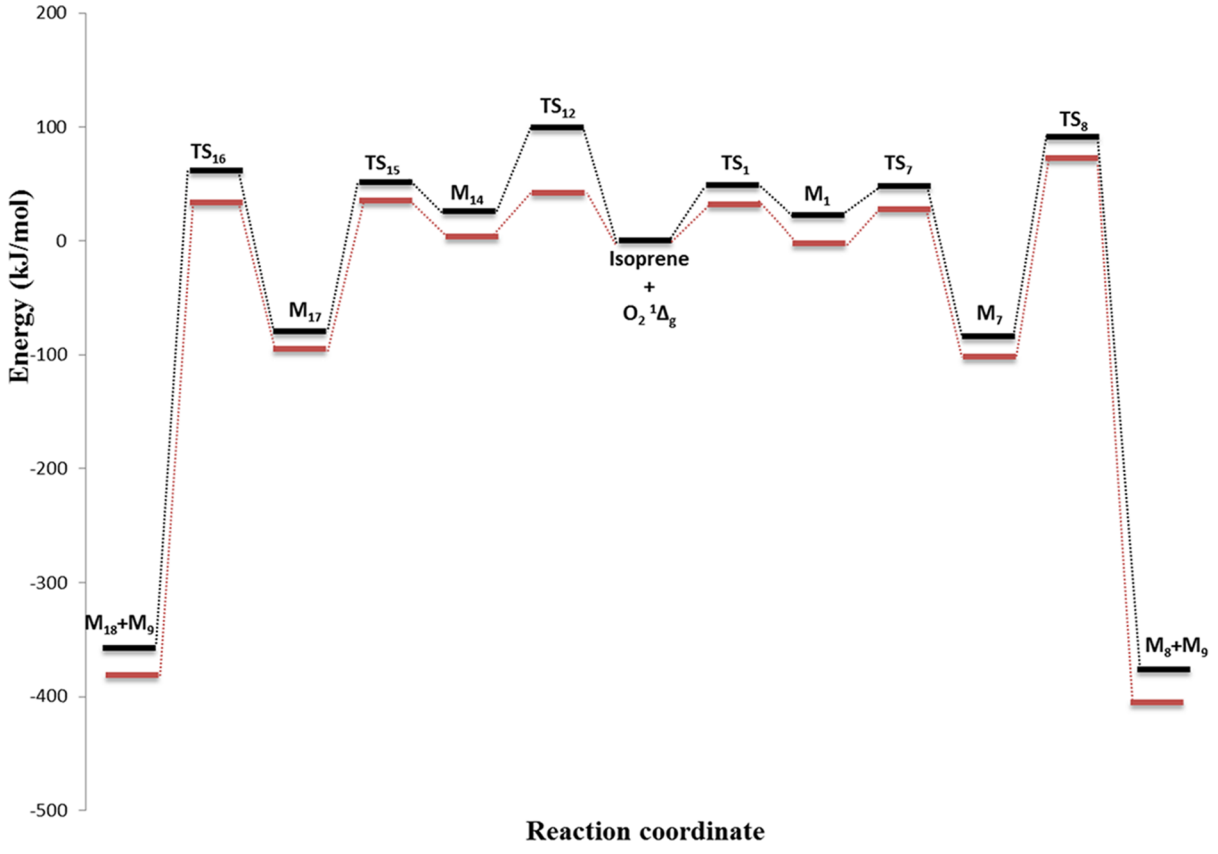

Figure 4. Potential energy diagram of isoprene + O_2 $^1\Delta_g$ reaction with (red) and without (black) solvent (water) effects.

DOI: 10.1021/acsomega.6b00025
ACS Omega 2016, 1, 220−225

($M_1 \rightarrow M_7 \rightarrow M_8 + M_9$). All other channels display negligible importance, including isomerization of M_1 into the six-membered cyclic peroxide M_{11}.

To investigate the solvent effect on the reaction energetics for the two main pathways (i.e., formation of M_8 and M_{18} from M_1 and M_{14}, respectively), we deploy a polarizable continuum model (PCM)[27] at the B3LYP/6-311g+(d,p) level of theory. Figure 4 contrasts the energies obtained in the gaseous and aqueous media. The PCM approach simulates the solvent effect by generating multiple overlapping spheres inside of a dielectric continuum, around the atoms within the molecule. The PCM predicts a systematic energy reduction in the range of 10 kJ/mol (TS_1) to 56 kJ/mol (TS_{12}) for transition states, intermediates, and final products along the two primary channels. Overall, the effect of the solvent is limited to reducing the energy penalties whereas the product distribution (i.e., based on kinetic values in Table 1) remains unchanged with reference to the gas-phase system.

Methyl vinyl ketone also constitutes a major product from the OH-initiated atmospheric oxidation of isoprene.[28] However, in accordance with the experimental finding of Jardine et al.,[11] we have shown that methyl vinyl ketone also appears from a within-plant oxidation of isoprene with O_2 $^1\Delta_g$. As Jardine et al.[11] have indicated, this calls for a reconsideration of the biogenic life cycle of isoprene and its oxidation products. Clearly, plants devote a significant effort into their protection against O_2 $^1\Delta_g$ by producing isoprene in a diurnal cycle[29] that reflects the formation of O_2 $^1\Delta_g$, in spite of the appearance of the cytotoxic methyl vinyl ketone as the reaction product.

■ ASSOCIATED CONTENT

Supporting Information

The Supporting Information is available free of charge on the ACS Publications website at DOI: 10.1021/acsomega.6b00025.

Table S1 (thermal enthalpies and spin contamination values for all species), Figures S1 (geometries of stable products and adducts), and Figure S2 (geometries of transition structures) (PDF)

■ AUTHOR INFORMATION

Corresponding Author

*E-mail: m.altarawneh@murdoch.edu.au. Phone: (+61) 8 9360 7507.

Notes

The authors declare no competing financial interest.

■ ACKNOWLEDGMENTS

This study has been supported by grants of computing time from the National Computational Infrastructure (NCI) and from the Pawsey Supercomputing Centre, Australia, as well as funds from the Australian Research Council (ARC). N.Z. and J.A.-N. thank Murdoch University for the award of post-graduate scholarships.

■ REFERENCES

(1) Guenther, A. Atmospheric chemistry: Are plant emissions green? *Nature* **2008**, *452*, 701−702.

(2) (a) Claeys, M.; Graham, B.; Vas, G.; Wang, W.; Vermeylen, R.; Pashynska, V.; Cafmeyer, J.; Guyon, P.; Andreae, M. O.; Artaxo, P.; Maenhaut, W. Formation of Secondary Organic Aerosols Through Photooxidation of Isoprene. *Science* **2004**, *303*, 1173−1176. (b) Fuentes, J. D.; Gu, L.; Lerdau, M.; Atkinson, R.; Baldocchi, D.; Bottenheim, J. W.; Ciccioli, P.; Lamb, B.; Geron, C.; Guenther, A.; Sharkey, T. D.; Stockwell, W. Biogenic Hydrocarbons in the Atmospheric Boundary Layer: A Review. *Bull. Am. Meteorol. Soc.* **2000**, *81*, 1537−1575.

(3) (a) Sharkey, T. D.; Wiberley, A. E.; Donohue, A. R. Isoprene Emission from Plants: Why and How. *Ann. Bot.* **2008**, *101*, 5−18. (b) Vickers, C. E.; Gershenzon, J.; Lerdau, M. T.; Loreto, F. A Unified Mechanism of Action for Volatile Isoprenoids in Plant Abiotic Stress. *Nat. Chem. Biol.* **2009**, *5*, 283−291.

(4) Sharkey, T. D.; Singsaas, E. L. Why Plants Emit Isoprene. *Nature* **1995**, *374*, 769.

(5) Monson, R. K.; Jones, R. T.; Rosenstiel, T. N.; Schnitzler, J.-P. Why Only Some Plants Emit Isoprene. *Plant, Cell Environ.* **2013**, *36*, 503−516.

(6) Triantaphylidès, C.; Havaux, M. Singlet Oxygen in Plants: Production, Detoxification and Signaling. *Trends Plant Sci.* **2009**, *14*, 219−228.

(7) Triantaphylidès, C.; Krischke, M.; Hoeberichts, F. A.; Ksas, B.; Gresser, G.; Havaux, M.; Van Breusegem, F.; Mueller, M. J. Singlet Oxygen is the Major Reactive Oxygen Species Involved in Photooxidative Damage to Plants. *Plant Physiol.* **2008**, *148*, 960−968.

(8) Tingey, D. T.; Manning, M.; Grothaus, L. C.; Burns, W. F. The Influence of Light and Temperature on Isoprene Emission Rates from Live Oak. *Physiol. Plant.* **1979**, *47*, 112−118.

(9) (a) Affek, H. P.; Yakir, D. Protection by Isoprene Against Singlet Oxygen in Leaves. *Plant Physiol.* **2002**, *129*, 269−277. (b) Velikova, V.; Edreva, A.; Loreto, F. Endogenous Isoprene Protects Phragmites Australis Leaves Against Singlet Oxygen. *Physiol. Plant.* **2004**, *122*, 219−225. (c) Loreto, F.; Velikova, V. Isoprene Produced by Leaves Protects the Photosynthetic Apparatus against Ozone Damage, Quenches Ozone Products, and Reduces Lipid Peroxidation of Cellular Membranes. *Plant Physiol.* **2001**, *127*, 1781−1787.

(10) Pyryaeva, A. P.; Goldort, V. G.; Kochubei, S. A.; Baklanov, A. V. Singlet Oxygen $O_2(^1\Delta_g)$ Formation via UV-Excitation of Isoprene-Oxygen $C_5H_8-O_2$ Encounter Complexes in Gas Phase. *Chem. Phys. Lett.* **2014**, *610*−*611*, 8−13.

(11) Jardine, K. J.; Monson, R. K.; Abrell, L.; Saleska, S. R.; Arneth, A.; Jardine, A.; Ishida, F. Y.; Serrano, A. M. Y.; Artaxo, P.; Karl, T.; Fares, S.; Goldstein, A.; Loreto, F.; Huxman, T. Within-Plant Isoprene Oxidation Confirmed by Direct Emissions of Oxidation Products Methyl Vinyl Ketone and Methacrolein. *Global Change Biol.* **2012**, *18*, 973−984.

(12) Clennan, E. L.; Pace, A. Advances in Singlet Oxygen Chemistry. *Tetrahedron* **2005**, *61*, 6665−6691.

(13) (a) Abe, M. Diradicals. *Chem. Rev.* **2013**, *113*, 7011−7088. (b) Bobrowski, M.; Liwo, A.; Ołdziej, S.; Jeziorek, D.; Ossowski, T. CAS MCSCF/CAS MCQDPT2 Study of the Mechanism of Singlet Oxygen Addition to 1,3-Butadiene and Benzene. *J. Am. Chem. Soc.* **2000**, *122*, 8112−8119.

(14) Yamanaka, S.; Kawakami, T.; Nagao, H.; Yamaguchi, K. Effective Exchange Integrals for Open-Shell Species by Density Functional Methods. *Chem. Phys. Lett.* **1994**, *231*, 25−33.

(15) (a) Datta, S. N.; Trindle, C. O.; Illas, F. *Theoretical and Computational Aspects of Magnetic Organic Molecules*; Imperial College Press: Singapore, 2014; pp 1−335. (b) Saito, T.; Nishihara, S.; Kataoka, Y.; Nakanishi, Y.; Kitagawa, Y.; Kawakami, T.; Yamanaka, S.; Okumura, M.; Yamaguchi, K. Reinvestigation of the Reaction of Ethylene and Singlet Oxygen by the Approximate Spin Projection Method. Comparison with Multireference Coupled-Cluster Calculations. *J. Phys. Chem. A* **2010**, *114*, 7967−7974.

(16) (a) Cramer, C. J.; Thompson, J. Quantum Chemical Characterization of Singlet and Triplet Didehydroindenes. *J. Phys. Chem. A* **2001**, *105*, 2091−2098. (b) Gräfenstein, J.; Cremer, D. The combination of density functional theory with multi-configuration methods—CAS-DFT. *Chem. Phys. Lett.* **2000**, *316*, 569−577.

(17) Montgomery, J. A.; Ochterski, J. W.; Petersson, G. A. A Complete Basis Set Model Chemistry. IV. An Improved Atomic Pair Natural Orbital Method. *J. Chem. Phys.* **1994**, *101*, 5900−5909.

DOI: 10.1021/acsomega.6b00025
ACS Omega 2016, 1, 220−225

(18) Frisch, M. J.; Trucks, G. W.; Schlegel, H. B.; Scuseria, G. E.; Robb, M. A.; Cheeseman, J. R.; Scalmani, G.; Barone, V.; Mennucci, B.; Petersson, G. A.; et al. *Gaussian 09*, A.1; Gaussian, Inc: Wallingford, CT, 2009.
(19) Mokrushin, V.; Bedanov, V.; Tsang, W.; Zachariah, M.; Knyazev, V. *ChemRate*, V.1.19; NIST: Gaithersburg, MD, 2002.
(20) Fukui, K. Role of Frontier Orbitals in Chemical Reactions. *Science* **1982**, *218*, 747−754.
(21) Hirshfeld, F. L. Bonded-Atom Fragments for Describing Molecular Charge Densities. *Theor. Chim. Acta* **1977**, *44*, 129−138.
(22) Delley, B. From Molecules to Solids with the DMol^3 Approach. *J. Chem. Phys.* **2000**, *113*, 7756−7764.
(23) Leach, A. G.; Houk, K. N. Diels−Alder and Ene Reactions of Singlet Oxygen, Nitroso Compounds and Triazolinediones: Transition States and Mechanisms from Contemporary Theory. *Chem. Commun.* **2002**, 1243−1255.
(24) Maranzana, A.; Ghigo, G.; Tonachini, G. Diradical and Peroxirane Pathways in the [π2+ π2] Cycloaddition Reactions of $^1\Delta$g Dioxygen with Ethene, Methyl Vinyl Ether, and Butadiene: A Density Functional and Multireference Perturbation Theory Study. *J. Am. Chem. Soc.* **2000**, *122*, 1414−1423.
(25) Bobrowski, M.; Liwo, A.; Ołdziej, S.; Jeziorek, D.; Ossowski, T. CAS MCSCF/CAS MCQDPT2 Study of the Mechanism of Singlet Oxygen Addition to 1,3-Butadiene and Benzene. *J. Am. Chem. Soc.* **2000**, *122*, 8112−8119.
(26) Luo, Y.-R. *Handbook of Bond Dissociation Energies in Organic Compounds*; CRC Press, 2002.
(27) Barone, V.; Cossi, M.; Tomasi, J. A New Definition of Cavities for the Computation of Solvation Free Energies by the Polarizable Continuum Model. *J. Chem. Phys.* **1997**, *107*, 3210−3221.
(28) Biesenthal, T. A.; Shepson, P. B. Observations of Anthropogenic Inputs of the Isoprene Oxidation Products Methyl Vinyl Ketone and Methacrolein to the Atmosphere. *Geophys. Res. Lett.* **1997**, *24*, 1375−1378.
(29) Warneke, C.; Holzinger, R.; Hansel, A.; Jordan, A.; Lindinger, W.; Pöschl, U.; Williams, J.; Hoor, P.; Fischer, H.; Crutzen, P. J.; Scheeren, H. A.; Lelieveld, J. Isoprene and Its Oxidation Products Methyl Vinyl Ketone, Methacrolein, and Isoprene Related Peroxides Measured Online over the Tropical Rain Forest of Surinam in March 1998. *J. Atmos. Chem.* **2001**, *38*, 167−185.

DOI: 10.1021/acsomega.6b00025
ACS Omega 2016, 1, 220−225